Catching CO_2 pollutant gas through nanocomposite formed by chitosan with non-circular C_{16} carbon double ring: VAMP study

J. H. Pacheco-Sánchez

Tecnológico Nacional de México, Instituto Tecnológico de Toluca, División de Estudios de Posgrado e Investigación, Av. Tecnológico S/N. Colonia Agrícola Bellavista, Metepec, Edo. de México, 52149 México.

F. J. Isidro-Ortega

Tecnológico Nacional de México, Instituto Tecnológico de Toluca, División de Estudios de Posgrado e Investigación, Av. Tecnológico S/N. Colonia Agrícola Bellavista, Metepec, Edo. de México, 52149 México.

I.-P. Zaragoza

Tecnológico Nacional de México, Campus Instituto Tecnológico de Tlalnepantla, Departamento de Eléctrica y Electrónica, Av. Mario Colín S/N, La Comunidad, Tlalnepantla de Baz, Edo. de México, 54700, México.

Received 19 April 2022; accepted 12 November 2022

VAMP study for catching CO_2 on nanocomposite generated by chitosan with non-circular C_{16} carbon ring, for contributing to distinguish the need for ambient air cleaning. Our aim is to modify porosity of chitosan as adsorbent of pollutant agents. At this time our searching is for taking profit of chitosan and carbon rings as new nanocomposite to be applied on air cleaning of pollutant gas, as it is carbon dioxide (CO_2). In here, a new material is proposed for pollutant gas capture to reduce atmospheric CO_2 levels. Particularly, C_{16} carbon double ring is responsible for catching CO_2, while on the one side chitosan is only capable to break CO_2 molecules, on the other side it can be surrounded by carbon ring molecules to catch more CO_2, pollutant molecules.

Keywords: Monomer chitosan copolymer; non-circular carbon ring; CO_2 pollutant gas; nanocomposite; VAMP study.

DOI: https://doi.org/10.31349/RevMexFis.69.031003

1. Introduction

Our aim in here is to get an improvement of chitosan as adsorbent of pollutant agents as CO_2 by modifying porosity in its structure, which can be changed to a nanocomposite by adding some form of carbon ring. This is important due to air pollution is a mixture of solid particles and gases in the air. Car emissions, chemicals from factories, dust, pollen, and mold spores suspended as particles, contribute to air pollution. We have previously been working using chitosan to clean water [1-10]. At this time our searching is for taking profit of chitosan and carbon rings as new nanocomposite to be applied for cleaning of air pollutant gas as carbon dioxide (CO_2). The capture of atmospheric carbon dioxide has increased due to a global increase in temperature. Atmospheric CO_2 levels have contributed to distinguish the need for ambient air cleaning. In this case a new material is proposed for pollutant gas capture. There are poisonous air pollutants as ozone gas, which is a major part of air pollution in cities. Ozone is a combination between pollution, heat, and sunlight, which is called smog. Among the effects of the air pollution in the environment are the following problems: global warming, climate change, acid rain, smog effect, deterioration of fields, extinction of animal species, respiratory health problems, deterioration in building materials.

Atmospheric carbon dioxide (CO_2) capture research has been increased due to a global rise in temperature. Levels of atmospheric CO_2 have contributed to distinguish need for capture processes. To reduce CO_2 emissions is a worldwide research matter, from emission sources as power plants burning fossil fuels, carbon capture and storage have been widely proposed [11]. The CO_2 capture has been achieved through chemical absorption (using aqueous amine solutions) for removing it from natural gas since long time ago [12]. Then, it is considered that already exists a technology readiness level (TRL) of 9. This technology use to be utilized in two post-combustion capture facilities in coal-fired power plants [13,14,15,16]. Advances in polymeric membranes have allowed technology to successfully reach demonstration scale (TRL 7). According to this, with our nanocomposite, new polymeric membranes might be constructed. Lithium orthosilicate is solid sorbent for capturing CO_2. Characteristics of the absorption reaction studied by thermogravimetric and volumetric methods exhibit influence of heat and mass transfer limitations in packed bed. This method measures absorption reaction characteristics in experiments. The CO_2 absorption rate depends on the CO_2 pressure and reactor temperature. The maximum absorption rate observed is at 670°C when the conversion fraction is 0.3 [17].

Nanoparticles (NP) prepared with chitosan and chitosan derivatives possess a positive surface charge and mucoadhesive properties such that can adhere to mucus membranes and release the drug payload in a sustained release manner. Chitosan-based NP have various applications i14n nonparenteral drug delivery for the treatment of cancer, gastrointestinal diseases, pulmonary diseases, drug delivery to the

brain and ocular infections according to the review [18]. Chitosan is a cationic biopolymer with potential applications in the food industry because of its unique nutritional and physiochemical properties. These properties depend on its ability to interact with anionic surface-active molecules, such as phospholipids, surfactants, and bile acids. [19]

Chitosan characteristics as adsorbent have been shown in literature. Monomer chitosan ($C_6H_{13}O_5N$) interacting with hBN nanosheet ($B_{48}N_{48}H_{24}$) in the armchair geometry with mono-hydrogenated ends yield chemisorption. The monomer is adsorbed parallel to the nanosheet inducing torsion in the nanosheet. The system at hand exhibits high polarity (3.076 D) like the interaction of chitosan and BN nanotube, and the amine group and hBN nanosheet as reported in literature [20]. The aflatoxins interaction with chitosan is computationally investigated by DFT-B3LYP functional with 6-31g(d) basis set. Through a total energy calculation, the most negative charge is on oxygen atoms of aflatoxins, being the preferred site to interact with chitosan. Aflatoxins are physisorbed and confirmed by the simulated IR spectra [21]. To represent the graphene or boron nitride nanosheet as a CnHm-like cluster to study the adsorption of the monomer of chitosan, represented by the monomeric unit ($C_6H_{13}O_5N$), on the graphene surface (G + MCh). As another case, the adsorption of MCh on the G nanosheet functionalized with boron (G + B) has been explored [20,22-25].

The nanocomposite is built joining one carbon double ring to one unit of copolymer chitosan. It is well known that geometry optimization of two parallel linear carbon chains of same size provide one polygonal carbon ring after interaction of these two chains [26]. A carbon double ring molecule appears in this case, for two parallel C_8 linear carbon chains interacting due to the initial chirality. According to the chirality and the size of carbon chains, more number of rings might appear, and only one when these stay parallel at 1.54 Å of separation.

2. Methodology

VAMP software in BIOVIA Materials Studio is a semiempirical method for calculating the heat of formation at 298°K, in contrast to ab initio methods, which compute electronic energy. The heat of formation is determined from a combination of computed and parameterized data as discussed by Stewart [27], and it is obtained using VAMP for a molecular configuration geometry which depends on computational parameters. After building a structure, it needs refining for getting a stable geometry [27-29].

Geometry optimization is applied using gradient norm of 0.4 kcal/mol/Å, partial general Hessian, Hamiltonian NDDO-AM1, spin restricted Hartree Fock, and CISD configuration interaction type. Using this methodology, and according to single point calculations shown in Fig. 1, the calculated energy for breaking one oxygen from CO_2 molecule is 147.28 kcal/mol while the experimental value of the dissociation energy (O-CO) of the CO_2 molecule is 125.749 kcal/mol

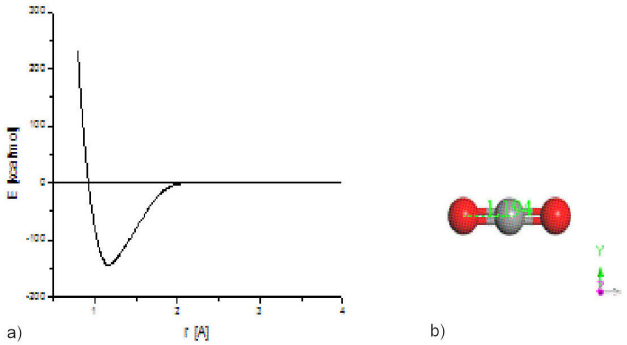

FIGURE 1. a) Potential energy curve for OELUMO-CO breaking, showing the size of the well of potential. b) OCO after geometry optimization. Oxygen atoms in red color, and carbon atom in gray color.

[30]. The difference corresponds to 14.6 %. On the other hand, frequency calculation for geometry optimization accomplished on a CO_2 molecule gives four vibrational normal modes:

<> Heat of Formation : -79.820491 kcal/mol

<> Zero Point Energy : 7.459 kcal/mol

<> Translations and Rotations (cm^{-1})

$$0.0345 = Tx \quad -0.0292 = Ty \quad 532.7572 = Tz$$

$$52.4078 = R1 \quad 53.7798 = R2$$

Vibration	Frequency (cm^{-1})	Reduced Mass	Raman Intensity
1	532.48	6.5245	0.0000
2	1480.17	7.9997	0.0000
3	2565.81	6.5214	0.0000
4	-0.02	0.0000	11.5438

The heat of formation 79.82 kcal/mol obtained using frequency calculations does not near of the experimental value with 36.52 % of error; however, frequency values converted from cm^{-1} to kcal/mol (532.48=1.52, 1480.17=4.23 and 2565.81=7.34) stay in the physisorption region.

Along with the previous frequency calculation, frontier orbitals HOMO and LUMO are obtained as another option in the properties of this VAMP methodology. $HOMO\ LUMO$ orbitals have been used in here to propose reaction sites for facilitating the corresponding chemical reactions. Gap HOMO-LUMO energy (14.04 eV) in one CO_2 molecule indicates a stable system and little reactive (see Fig. 2).

Calculations are carried out using cero global charge. However, as an example a comparison between Coulson and Mulliken atomic charges for the C_{16} carbon double ring obtained after geometry optimization of two carbon chains as input (see Fig. 3) are shown in Tables I and II.

TABLE I. Coulson atomic charges.

Atom	Type	Charge	Atom	Type	Charge
1	C	0.025	2	C	0.093
3	C	0.131	4	C	0.068
5	C	0.008	6	C	0.009
7	C	0.006	8	C	0.000
9	C	0.024	10	C	0.092
11	C	0.131	12	C	0.068
13	C	0.009	14	C	0.009
15	C	0.007	16	C	0.001

TABLE II. Mulliken atomic charges.

Atom	Type	Charge	Atom	Type	Charge
1	C	-0.000	2	C	-0.074
3	C	0.125	4	C	-0.056
5	C	0.013	6	C	-0.009
7	C	0.006	8	C	-0.003
9	C	-0.001	10	C	-0.074
11	C	0.125	12	C	-0.057
13	C	0.013	14	C	-0.009
15	C	0.006	16	C	-0.004

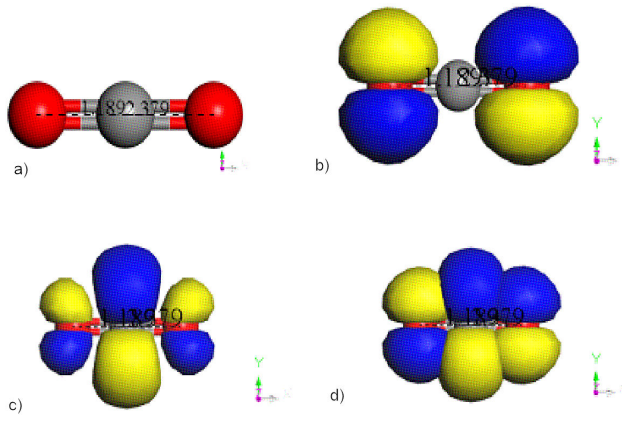

FIGURE 2. Energy of $HOMO - LUMO$ on a CO_2 molecule. a) CO_2 molecule of size 2.379 Å. b) $E_{HOMO} = -13.211$ eV c) $E_{LUMO} = 0.853$ eV d) Gap $(E_{LUMO} - E_{HOMO}) = 14.04$ eV.

By symmetry in the C_{16} carbon double ring, we see that atoms 1 and 9, 2 and 10, and so on, have very similar charges, both for the Coulson and Mulliken atomic charge. In both cases the largest charge corresponds to atoms 3 and 11, while the smallest charge corresponds to charges 8 and 16 in the Coulson case, and 1 and 9 in the Mulliken case. Connectivity calculations according to Estrada inferences [31] on no bonding to $s-$ and $f-$shell scheme, bond type, and converting representation to Kekulé are accomplished for bond length tolerances from 0.6 to 1.15 Å.

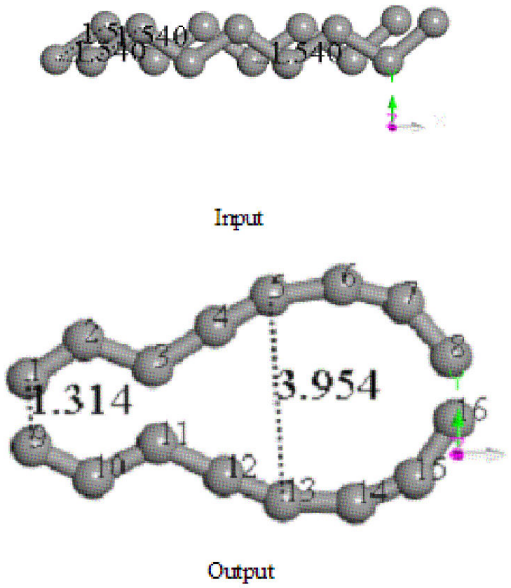

FIGURE 3. Input and output of the geometry optimization on two C_8 carbon chains. Two C_8-carbon chains separated at distance of one C−C bond length 1.54 Å.

3. Results and discussion

Two parallel C_8 single-bond carbon chains at a separation distance of 1.54 Å (the experimental value of C−C bond is 1.535 Å) have been set in the input for geometry optimization, as observed in Fig. 3 with certain chirality. After interaction of these carbon chains through geometry optimization (four times using the methodology mentioned previously), the output exhibits a carbon double ring, one C_6 ring and one non-circular C_{12} ring sharing one C−C single bond, on which after applying connectivity and bond type for no bonding to $s-$ and $f-$shell, the biggest ring is double bond, and the smallest ring has two triple and four single bonds (see Fig. 4).

Carbon rings alternating single and triple bonds $(-C\equiv C-)_n$ are known as carbyne or acetylenic structures, however, when only double bonds are present $(=C=C=)_n$ [32,33] cumulenic structures are formed. In this case, this carbon double ring alternates carbyne and cumulene rings.

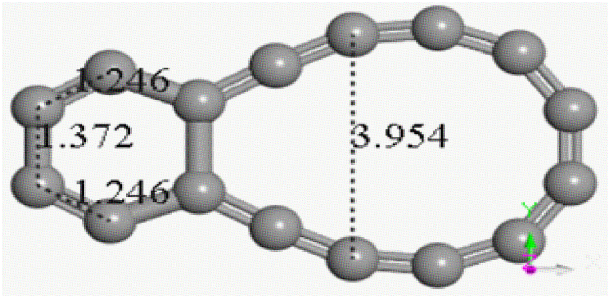

FIGURE 4. Conectivity applied on the output of Fig. 3. C_{16} carbon double ring (C_6 and C_{12}) sharing one bond length after geometry optimization. Gray color for carbon atoms.

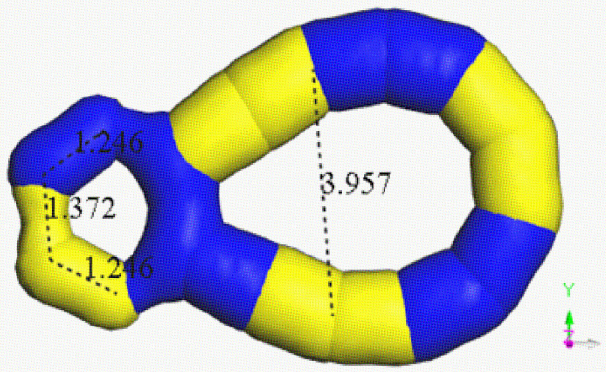

FIGURE 5. $HOMO - LUMO$ of this C_{16} carbon double ring, two joined (C_6-C_{12}) carbon rings.

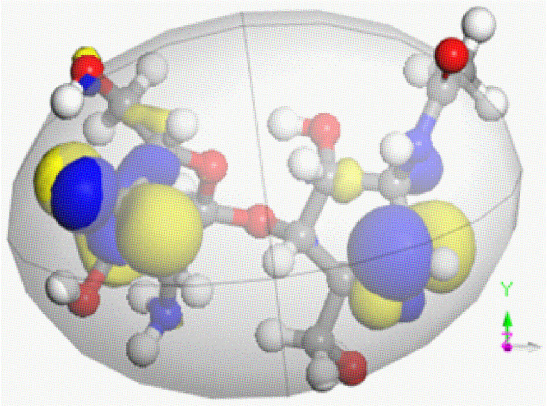

FIGURE 7. Output: HOMO-LUMO of the bonding and antibonding places.

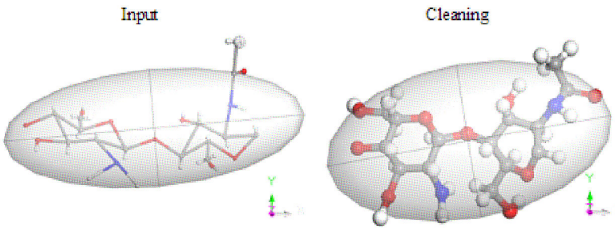

FIGURE 6. Input: Building a copolymer chitosan structure plus a rough cleaning. Gray, white, red, and blue color for carbon, hydrogen, oxygen, and nitrogen atoms, respectively.

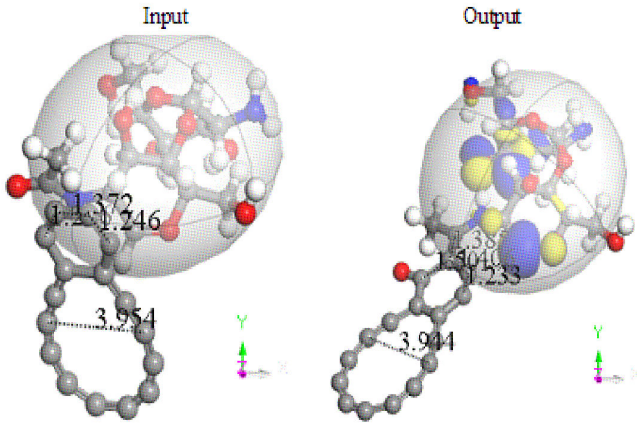

FIGURE 8. Input-Output about geometry optimization on interaction between chitosan and carbon double ring, with the C_6 carbon ring bonded to chitosan at the end.

The heat of formation of the C_{16} carbon double ring is 669.41468 kcal/mol. The output is also calculated to show the $HOMO - LUMO$ for bonding (blue orbitals) and antibonding (yellow orbitals), thus, as it can be seen in Fig. 5, blue bonds between atoms in the molecule are the places for insertion of other atoms of another molecule according to the electron sharing between them.

To continuation a sketch of one unit of copolymer chitosan ($C_{14}H_{24}N_2O_9$) has been built to be taken as Input for geometry optimization, on which cleaning has been applied as first approximation to bond lengths and angles, as shown in Fig. 6.

After this, the Output of geometry optimization using VAMP is accomplished. This result exhibits $HOMO - LUMO$ for the corresponding bonding and antibonding places, as shown in Fig. 7. Such molecular structure has: Chemical Formula = $C_{14}H_{24}N_2O_9$, NetMass = 364.351, NumAtoms = 49, NetCharge = 0.00000 e, $E_{HOMO} = -6.723$ eV (orbital 72), $E_{LUMO} = -3.893$ eV (orbital 73). Considering $E_{GAP} = E_{LUMO} - E_{HOMO}$, $E_{GAP} = 2.83$ eV. Then, we proceeded to use software 'Modify' from BIOVIA Materials Studio for applying 'Charges' with Initial charge = Formal, and Parameter set = $Q_{eq} - charged1.1$. After applying 'calculate' NetCharge = -6.0000 e, and the E_{GAP} calculation is still the same. This E_{GAP} corresponds to singlet of multiplicity due to Spin Down [34,35] for even electron number.

Then, to get a chitosan-carbon nanocomposite, these were put together in the input with a configuration on which one carbon atom of the non-circular carbon ring is close to a C−N bond length. A new configuration is obtained in the output, where the non-circular carbon ring is perpendicular to one unit of copolymer chitosan and one oxygen atom was captured by the non-circular carbon ring, and this whole system has been inserted into chitosan forming a nanocomposite with $C_{30}H24N_2O_9$ chemical formula. We see in the output of the geometry optimization (Fig. 8) the insertion of the C_{16} double carbon atom in the $C_{14}H_{24}N_2O_9$ copolymer molecule of chitosan which has been rotated 90° approximately. Chitosan has been modified because one of its oxygen atoms stays now adsorbed in the smallest ring of C_{16} carbon double ring. Then, the $C_{30}H24N_2O_9$ configuration of the chemical structure is the new product, which is one nanocomposite unit.

The adsorption when non-circular C_{12} carbon ring is the nearest one to chitosan copolymer, according to the output after geometry optimization remains as observed in Fig. 9 in two perspectives. This Figure clearly exhibits the facilities given by $HOMO - LUMO$ for providing reaction sites in this interaction, which in this case corresponds to attractive forces. Furthermore, this nanocomposite has: Chemical Formula = $C_{30}H_{24}N_2O_9$, NetMass = 556.527,

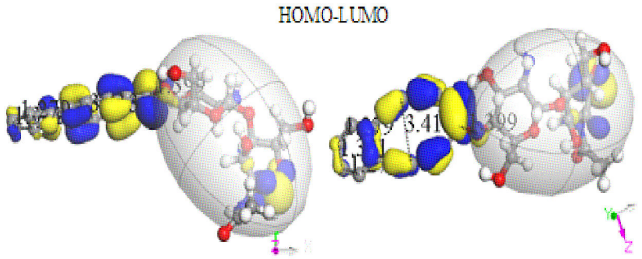

FIGURE 9. Two perspectives of geometry optimization on interaction between chitosan and carbon double ring, with the greatest ring bonded to chitosan in one side.

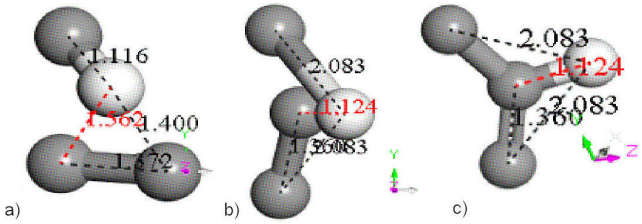

FIGURE 10. Interaction between reaction sites and of C_{16} carbon double ring and $C_{14}H_{24}N_2O_9$ copolymer chitosan, respectively. This notation implies that C_2 is part of the C_{16} carbon ring, and HC is part of the $C_{14}H_{24}N_2O_9$ chitosan molecule.

NumAtoms = 65, NetCharge = 0.00000 e, $E_{HOMO} = -6.952$ eV (orbital 104), $E_{LUMO} = -4.296$ eV (orbital 105), $E_{GAP} = E_{LUMO} - E_{HOMO} = 2.656$ eV corresponding to Spin Down and singlet of multiplicity due to the absence of electrons. By applying 'Charges' with Initial charge = Formal, and Parameter set = $Q_{eq\_charged}1.1.$, it results NetCharge = -5.0000 e, and $E_{GAP} = E_{LUMO} - E_{HOMO} = -4.258$ eV - (-6.96eV) = 2.702 eV. This E_{GAP} corresponds to Spin Up [34,35] due to odd number of electrons, and doublet of multiplicity.

To confirm that non-circular carbon ring is responsible of this chemical adsorption, we extract one of its interaction sites, which is the C−C carbon molecule in Fig. 10a). According to C−C bond length of Fig. 5, it has antibonding orbitals. The other part of Fig. 10a) has been extracted from Chitosan molecule. The whole Fig. 10a) has been extracted from the Input of Fig. 8, and it is now the Input on which a geometry optimization is applied, obtaining a new conformation shown in Fig. 10b). In the latter, we observe C−C bond as head on perpendicular to C−H bond length greater than the initial one C−C bond side on perpendicular to C−H, meaning that in Fig. 10b) one carbon atom of C−C is inserting in the bond of the C−H. Applying connectivity from BIOVIA MS Modeling, chemical adsorption is clearly observed in Fig. 10c).

Antibonding orbitals carry at to repulsive effects, then in Fig. 11, which exhibits orbitals of Fig. 10a), it is observed that bonding is located between C−H carbon atom and the bond length of C−C, as expected.

One CO_2 molecule can be independently captured by either C_{16} non-circular ring or $C_{14}H_{24}N_2O_9$ chitosan copolymer. An example of the former is shown in three steps of

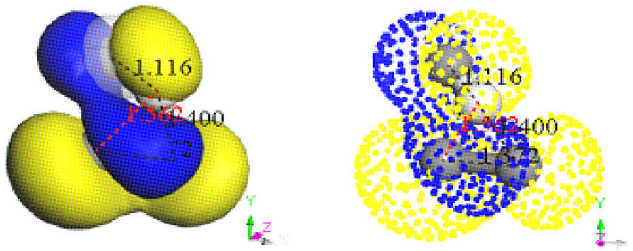

FIGURE 11. $HOMO - LUMO$ of Fig. 10a) in two perspectives.

Fig. 12 (input, output, and connectivity); however, in Fig. 12b), it is observed a potential energy curve of the conformation shown in Fig. 12a). This interaction between linear CO_2 with heat of formation of -99.029128 kcal/mol and planar C_{16} carbon double ring (having a heat of formation of 611.621 kcal/mol) considers rigid molecules and it exhibits a well of potential with a small size of energy around 2 kcal/mol as in Fig. 12b). The output in Fig. 12c) exhibits a conformation where the CO_2 is non-linear, given that it considers the same input of Fig. 12a), now with relaxed molecules, and Fig. 12d) exhibits the connectivity between the molecules in Fig. 12c), which is the insertion of CO_2 in the C_{16} carbon double ring. now with carbyne oxide $C_{17}O_2$ (with heat of formation of 535.445 kcal/mol) structure, due to the alternating single and triple bonds. The adsorption energy of Fig. 12a) is calculated as:

$$E_{\text{ad}}(\text{Heat of Formation}) = E_{C_{17}O_2} - E_{C_{16}} - E_{CO_2} = 22.853128 \text{ kcal/mol}. \quad (1)$$

In the latter result for a relaxed optimization, the heat of formation provides a chemisorption, while the rigid case provides a physisorption, according to the range handled by

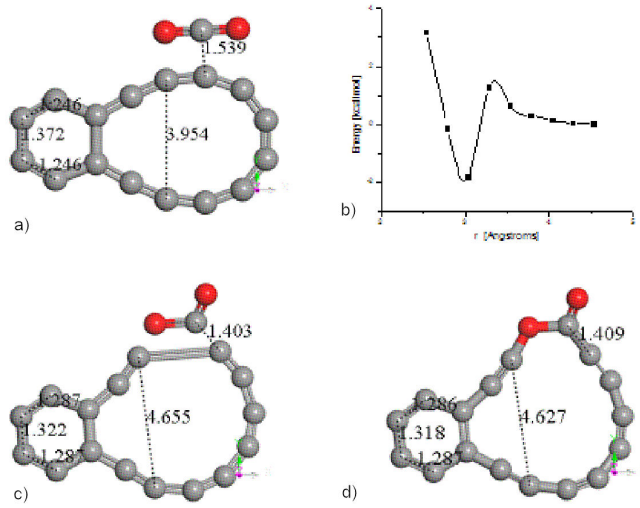

FIGURE 12. CO_2 attacking C_{16} carbon double ring. a) Input, for geometry optimization, b) Interaction for the previous configuration, c) Output, of the geometry optimization, d) Connectivity.

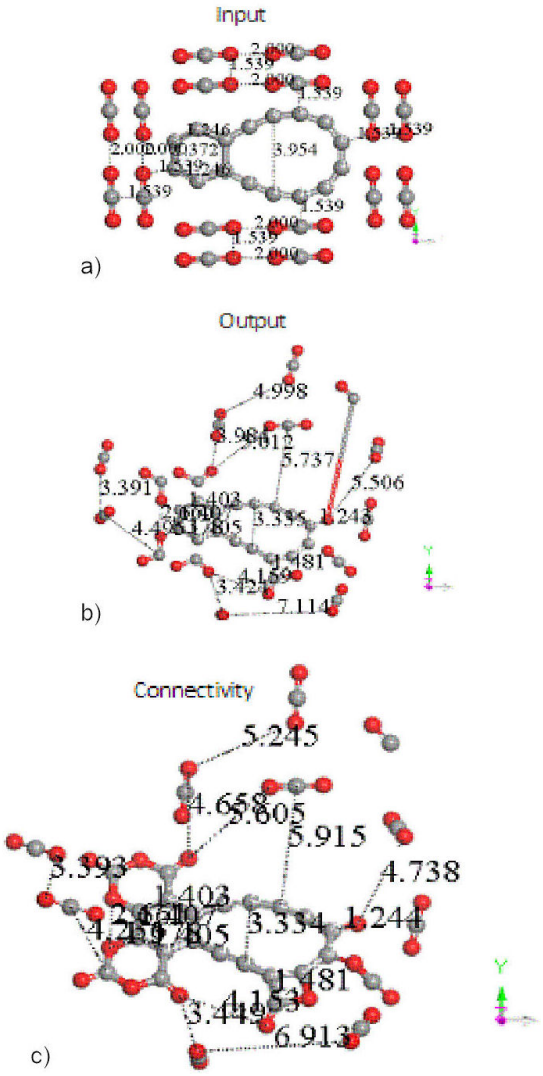

FIGURE 13. C_{16} carbon double ring is attacked by 16 CO_2 molecules. After minimum energy optimization around 50% of CO_2 molecules are adsorbed on C_{16} carbon double ring.

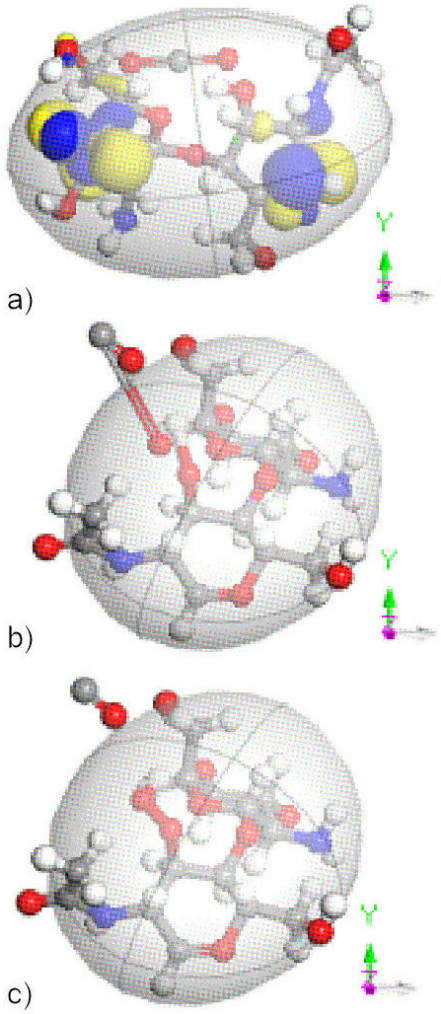

FIGURE 14. Carbon dioxide CO_2 attacking $C_{14}H_{24}N_2O_9$ chitosan copolymer. a) Input, b) Output, c) Connectivity.

Atkins [36] and others [37-39], around 5 kcal/ mol for physisorption and greater than 10 kcal / mol for chemisorption, approximately because it depends on the elements in the system. Then, through chemisorption CO_2 is captured by C_{16} forming a new $C_{17}O_2$ molecule as observed in Fig. 12.

In case of more than one CO_2 molecules interacting with C_{16} carbon double ring, in an input arrangement to the geometry optimization shown in Fig. 13a), we see in the output for the geometry optimization shown in Fig. 13b), that at least 50% of CO_2 gas are molecules adsorbed on this carbon ring, and the other 50% CO_2 molecules have been repulsed when 16 CO_2 molecules interact with C_{16} carbon double ring as shown in Fig. 13c). The input exhibits a separation of 1.539Å between CO_2 molecules in a geometrical ordered arrangement. The electrostatic attractions and repulsions among these molecules provide around 50 % of CO_2 molecules tending to move away, and three carbon rings added to the C_{16} carbon double ring. Then a new molecule of five rings has one carbon ring of ten atoms and another of six atoms, two new rings of six and one more new ring of four atoms. The latter has one oxygen and three carbon atoms, and in the two new rings of six atoms there are two oxygen atoms alternating with carbon atoms as shown in Fig. 13c). One carbon dioxide molecule is broken in an oxygen atom which stay bonded to the C_{16} carbon double ring molecule, and a CO molecule moves away, consequently there is certain percentage of formation of carbon monoxide, while the carbon dioxide considerably decreases as pollutant.

An example of interaction between one molecule of CO_2 and one molecule of copolymer chitosan is shown also in three steps in Fig. 14 (input, output, and connectivity): From these two cases using VAMP calculations, while CO_2 is captured by carbon double ring in the former, in the latter CO_2 is broken giving CO as new product. Then, among reactions between CO_2 and the nanocomposite $C_{30}H_{24}N_2O_9$, the CO_2 can be captured near to carbon atoms, and can be broken near to gas atoms.

4. Conclusions

The multiplicity of one unit of $Chitosan-copolymer+C_{16}$ carbon double ring is singlet for NetCharge = 0.0000 e, while it is doublet when NetCharge = -5.0000. The latter corresponds to cationic character of chitosan. Considering $E_{GAP}\uparrow$ and $E_{GAP}\downarrow$ as gap energy of spin up and spin down, respectively, the difference between them is $E_{GAP}\uparrow -E_{GAP}\downarrow = 0.046$ eV.

Carbon dioxide CO_2 molecules can be adsorbed by either nanocomposite or independently by C_{16} double-carbon-ring or copolymer chitosan. The confidence of this semiempirical model in this case is about 15 % due to the comparison between experimental dissociation energy of CO_2 and the breaking of one oxygen atom from the CO_2 molecule.

The generated $C_{30}H_{24}N_2O_9$ nanocomposite has an improved superficial area with respect to the pristine either C_{16} or $C_{14}H_{24}N_2O_9$, and for increasing CO_2 catching. In this case, the C_{16} carbon molecule is that acting to degrade the oxygen atoms in molecules such as CO_2. Then, as much carbon molecules added to the copolymer the better is the adsorption of CO_2 in nanocomposite of this composition, given that porosity of chitosan has been changed to be adsorbent of pollutant agents.

We applied different methodologies with different results on the size of the carbon double ring. However, with the chosen Hamiltonians, it seems as if C_{16} carbon double ring were activated in the insertion process on a chitosan unit, which promotes it to be in charge for catching CO_2, because the results for catching CO_2 on chitosan indicate that repulsion is easier than attraction.

Acknowledgements

IPZR The authors gratefully acknowledge the financial support of their project TecNM. No. 8252.20-P.

1. R. Suárez and J. Pacheco, Estudio DFT: Adsorción de cobre doblemente ionizado por el grupo amino del quitosano, Revista de Simulación y Laboratorio, **4**(13) (2017) 46, ISSN: 2410-3462
2. R. Suárez-Reyes, I. P. Zaragoza, J.H. Pacheco-Sánchez, BOMD study on the reaction among one amaranth dye molecule and one chitosan repetitive unit, *Mediterranean Journal of Chemistry*, **7** (2018) 243-252, http://dx.doi.org/10.13171/mjc74181104-zaragoza
3. J. H. Pacheco-Sánchez, Some Pollutants to Defeat to get Clean Drinking Water, American *Journal of Biomedical Science & Research*, **4** (2019) 429-430 http://dx.doi.org/10.34297/AJBSR.2019.04.000848
4. J.H. Pacheco Sánchez and R. Suárez Reyes, A DFT Study for Eliminating a Water Pollutant by Using an Adsorbent, *American Journal of Biomedical Science & Research*, **7** (2020) 345-349 https://doi.org/10.34297/AJBSR.2020.07.001174.
5. D. Hernández-Benitez and J. H. Pacheco-Sánchez, Optimization of Chitosan+Activated Carbon Nanocomposite. DFT Study, **3** (2018) 436-448 Archives of Organic and Inorganic Chemical Sciences https://doi.org/10.32474/AOICS.2018.03.000175.
6. J. H. Pacheco-Sánchez, Chitosan Copolymer with Activated Carbon as Nanocomposite Through DFT Modeling, American Journal of Biomed Science & Research, **4** (2019) 404-409 https://doi.org/10.34297/AJBRS.2019.04.000843
7. J. H. Pacheco-Sánchez, B. García-Gaitán, R. Suárez-Reyes, R. E. Zavala-Arce, Neutral Acid Form of the Complex Molecule Among Chitosan and Azoic Dye Reaction Sites, XXVIII Congreso Nacional de la Sociedad Polimérica de México, San Miguel de Allende, GTO, Noviembre, **4** (2015) 96-101, ISSN: 2448-6272
8. J. H. Pacheco Sánchez, B. García Gaitán, R.E. Zavala Arce, A DFT Study Among Interaction Sites: of Polimeric Chitosan and of Azoic Colorant Red 2, Polymer Meeting MACROMEX, Nuevo Vallarta, Nayarit Diciembre, **3** (2014) 402-407, ISSN: 2448-6272
9. J.I. Moreno-Puebla, C. Hernández-Tenorio, B. García Gaitán, J. L. García-Rivas, R.E. Zavala Arce, J.H. Pacheco Sánchez, Evaluation of the Adsorption of Red 2 Dye in Aqueous Solutions Using Chitosan-Cellulose Hydrogel Beads, Polymer Meeting MACROMEX, Nuevo Vallarta, Nayarit Diciembre, **3** (2014) 466-470, ISSN: 2448-6272
10. J.N. Balderas-Gutiérrez, C. Hernández-Tenorio, R. E. Zavala-Arce, J.H. Pacheco-Sánchez, B. García-Gaitán, J. Illescas, Chitosan films modified with glow discharge plasma in aqueous solution of pyrrole and its evaluation in the removal of red dye no. 2, Revista Mexicana de Ingeniería Química, **19** (2020) 1291, https://doi.org/10.24275/rmiq/IA893
11. M. Bui, *et al*., Carbon capture and storage (CCS): the way forward, *Energy & Environmental Science*, **11** (2018) 1062-1176, https://doi.org/10.1039/C7EE02342A
12. R. R. Bottoms, US Pat., application 1783901, (1930)
13. M. Campbell, Technology innovation & advancements for shell cansolv CO_2 capture solvents, *Energy Procedia*, **63** (2014) 801-807, https://doi.org/10.1016/j.egypro.2014.11.090
14. A. Singh and K. Stéphenne, Shell Cansolv CO2 capture technology: Achievement from First Commercial Plant, *Energy Procedia*, **63** (2014) 1678-1685, https://doi.org/10.1016/j.egypro.2014.11.177
15. Petra Nova - W.A. Parish Project, Office of Fossil Energy, (U.S. Department of Energy (DOE)), https://doi.org/10.1007/s11671-008-9136-2http://energy.gov/fe/petra-nova-wa-parish-project

16. Petra Nova W.A. Parish Fact Sheet: Carbon Dioxide Capture and Storage Project, Carbon Capture and Sequestration, (Technologies program at MIT, 2016), https://sequestration.mit.edu/tools/projects/wa_parish.html

17. T Esaki, D Iwase, and N Kobayashi, Evaluation of Carbon Dioxide Absorption Characteristics Lithium Ortho-Silicate in Chemical Heat Storage, *Journal of Materials Science and Chemical Engineering*, **5** (2017) 56-63. https://doi.org/10.4236/msce.2017.54006

18. A Munawar Mohammed, Jaweria T. M. Syeda, Kishor M. Wasan, and Ellen K. Wasan, An Overview of Chitosan Nanoparticles and Its Application in Non-Parenteral Drug Delivery, *Pharmaceutics*, **9** (2017) 53, https://doi.org/10.3390/pharmaceutics9040053

19. M Thongngam, DJ McClements, Characterization of interactions between chitosan and an anionic surfactant, *J Agric Food Chem*, **52** (2004) 987-91, https://doi.org/10.1021/jf034429w

20. E. Chigo Anota, L. D. Hernández Rodríguez, and G. Hernández Cocoletzi, Influence of Point Defects on the Adsorption of Chitosan on Graphene-Like BN Nanosheets, *Graphene*, **1**(2) (2013) 1-7, https://doi.org/10.1166/graph.2013.1014

21. L. A. Juárez-Morales, H. Hernández-Cocoletzi, E. Chigo-Anota, E. Águila-Almanza and M. G. Tenorio-Arvide, Chitosan-Aflatoxins B1, M1 interaction: A computational approach, *Current Organic Chemistry*, **21** (2017), https://doi.org/102174/1385272821666170511165159

22. E Chigo Anota, RE Ramírez Gutierrez, A Escobedo Morales, G Hernández Cocoletzi, Influence of point defects on the electronic properties of boron nitride nanosheets, *J Mol Model*, **18** (2012) 2175, https://doi.org/10.1007/s00894-011-1233-y

23. E Chigo Anota, A Escobedo Morales, M Salazar Vilanueva, O Vazquez Cuchillo, E Rubio Rosas, On the influence of point defects on the structural and electronic properties of graphenelike sheets: a molecular simulation study, J Mol Model, **19** (2013) 839, https://doi.org/10.1007/s00894-012-1612-z

24. E Chigo Anota, RE Ramírez Gutiérrez, FL Pérez Sánchez, JF Sánchez Ramírez, Structural characteristics and chemical reactivity of doped graphene nanosheets, Graphene, **1** (2013) 31-36, https://doi.org/10.1166/graph.2013.1008

25. E Chigo Anota, A Rodríguez Juárez, M Castro, H Hernández Cocoletzi, A density functional theory analysis for the adsorption of the amine group on graphene and boron nitride nanosheets, J Mol Model, **19** (2013) 321-328 https://doi.org/10.1007/s00894-012-1539-4

26. JH Pacheco-Sánchez, IP Zaragoza-Rivera, A Bravo-Ortega, Interaction of small carbon molecules and zinc dichloride: DFT study, Rev Mex Fís, **63** (2017) 97-110, https://repositorio.unam.mx/contenidos/4107435

27. JJP Stewart, MOPAC a special issue of J. Comput. - Aided Mol. Des., **4**, 1 (1990). https://doi.org/10.1007/BF0012833

28. JA Pople; DL Beveridge, Approximate Molecular Orbital Theory, (McGraw-Hill: New York 1970).

29. JA Pople, WJ Hehre, L Radom, P v R Schleyer, Ab Initio Molecular Orbital Theory, (J Wiley, NY 1986). ISBN: 978-0-471-81241-8

30. G. Herzberg, Molecular Spectra and Molecular Modeling, III Electronic Spectra and Electronic Structure of Poliatomic Molecules. (Krieger Publishing Company, FL 1966)

31. E. Estrada, Physicochemical interpretation of molecular connectivity indices, J. Phys. Chem. A, **106** (2002) 9085. https://doi.org/10.1021/jp026238m

32. Y.H. Hu, Stability of sp carbon (carbyne) chains, Physics Letters A, **373** (2009) 3554-3575, https://doi.org/10.1016/j.physleta.2009.07.067

33. M. Liu, V. I. Artyukhov, H. Lee, F. Xu and B. I. Yakobson, Carbyne from first principles: Chain of C atoms, a nanorod or a nanorope, ACSNano, **7** (2013) 10075-10082, https://doi.org/10.1021/nn404177r

34. Marcelo Galván, Alberto Vela, José L. Gázquez, Chemical Reactivity in Spin-Polarized Density Functional Theory, J. Phys. Chem., **92** (1988) 6470-6474. https://doi.org/10.1021/j100333a056

35. Y. Mo, Z. Lin, W. Wu, and Q. Zhang Delocalization in Allyl Cation, Radical, and Anion, J. Phys. Chem. **100** (1996) 6469-6474, https://doi.org/10.1021/jp9526612

36. P.W. Atkins, Physical Chemistry, (Oxford University Press, NY 2001)

37. A.M. Blas, Bs Thesis, ESIQIE Instituto Politécnico Nacional, México, 1981

38. R. A. Lobo, Aspectos fundamentales del desarrollo de procesos fisicoquímicos. SEP, UAM-I y UAZ, Zacatecas, Zac., Junio 1979.

39. Crini, G., Badot, P. M., Application of chitosan, a natural aminopolysaccharide, for dye removal from aqueous solutions by adsorption processes using batch studies: A review of recent literature, Progress in Polymer Science, **33** (2008) 399.